View metadata, citation and similar papers at core.ac.uk
brought to you by CORE
provided by Institute of Transport Research:Publications

Wind turbine stability: Comparison of state-of-the-art aeroelastic simulation tools

O Hach[1], H Verdonck[1], J D Polman[2], C Balzani[2], S Müller[3], J Rieke[3], H Hennings[1]

[1]German Aerospace Center, Institute of Aeroelasticity, Bunsenstr. 10, 37073 Göttingen, Germany
[2]Leibniz University Hannover, Institute for Wind Energy Systems, Appelstr. 9A, 30167 Hannover, Germany
[3]Nordex Energy GmbH, Langenhorner Chaussee 600, 22419 Hamburg, Germany

E-mail: oliver.hach@dlr.de

Abstract. As rotor diameters and blade flexibility are increasing, current and future generation wind turbines are more susceptible to aeroelastic instabilities. It is thus important to know the prediction capabilities of state-of-the-art simulation tools in regards of the onset of aeroelastic instability. This article presents results of a code-to-code comparison of five different simulation codes using a representative wind turbine model. It is shown that the models are in good agreement in terms of isolated structural dynamics and steady state aeroelastics. The more complex the test cases become, the more significant are the differences in the results. In the final step of comparison, the aeroelastic stability limit is determined through a run-away analysis. The instability onset is predicted at different wind speeds and the underlying mechanisms differ between the tools. A Campbell diagram is used to correlate the findings of time domain simulation tools with those of a linear analysis in the frequency domain.

1. Introduction

Increasing rotor diameter and a flexible blade structure are characteristic features of recent and future generations of wind turbines. Moreover, complex interactions between different turbine components and the environment result in challenging aeroelastic conditions [1]. Hence, the following question arises: Are current simulation tools comparable in their ability in predicting the aeroelastic behavior of wind turbines, especially considering aeroelastic stability?

A code-to-code comparison is a way to provide benchmark tests and verify the accuracy and correctness of different simulation codes. A comparison to note is the Offshore Code Comparison Collaboration for IEA Wind Task 23 [2]. Therein, simulation results are compared for the NREL 5 MW baseline wind turbine model [3] for different offshore support structures. In order to better understand the unsteady modeling of aerodynamics, simulations were also compared with wind tunnel experiments [4]. This blind code-to-code-to-measurements comparison showed large differences, e. g. in the prediction of power in detached unsteady wind conditions.

Experience in aircraft design has shown that aeroelastic instabilities became an issue as aircraft wings grew longer and became more flexible [5]. It can therefore be expected that today's rotor blades for multi-MW-sized wind turbines are more susceptible to aeroelastic instabilities [6, 7]. Hence, taking aeroelastic stability into account is state-of-the-art in wind

turbine aeroelasticity [8]. Traditionally, the aeroelastic stability problem is formulated in the frequency domain. The equations of motion are linearized with respect to a wind turbine state. The modes and frequencies which contribute to the turbine state are determined via an eigenvalue analysis. The rotation of the rotor with respect to the fixed ground frame can be taken into account with the Coleman transformation. In this way, many operational conditions can be analyzed in the context of aeroelastic stability [6, 9, 10, 11]. Alternatively, the Floquet analysis can be incorporated to account for the periodicity of the turbine state. Although this theory is computationally more expensive, it reveals multiple harmonics in the modes [12, 13]. Unsteady aerodynamics can also be taken into account in the frequency domain [7, 11].

An aeroelastic stability analysis in the time domain is less typical. However, non-linearities become increasingly important in modern wind turbines with tip deflections of more than 10 % of the blade length. These are easier to incorporate in a time domain analysis since an a priori linearization is not required. For example, the trailed vorticity can be taken into account which can lead to an increased flutter speed [14]. A run-away analysis is exceptionally attractive in this context due to its simplicity. Therein, the pitch controller and the generator torque are disabled, and the wind velocity is typically gradually increased. In this way, the rotor is allowed to accelerate freely. The resulting high tip speed ratios are usually avoided in the operation of wind turbines. However, the high relative inflow velocities can provoke aeroelastic instabilities, which is the goal of the run-away analysis.

The objective of the present paper is to benchmark state-of-the-art simulation tools for wind turbines in terms of the predicted aeroelastic stability. The study is carried out as a code-to-code comparison between two general purpose multibody system simulation codes (alaska/Wind[15] and Simpack [16]) and three simulation tools specifically dedicated to wind turbines (Bladed [17], HAWC2 [18], OpenFAST [19]) that are well established in research and/or industry.

The reference wind turbine model IWT-7.5-164 [20] with a rated power of 7.5 MW, a rotor diameter of 164 m and a blade arc length of 80 m is employed for this study, which was initially developed in the *SmartBlades* project [21]. The model and its adaptation for the different tools are briefly described in section 2. The first part of the comparison includes the verification of model comparability by a cross-check between the five simulation codes as presented in section 3. The second part in section 4 comprises the investigation of aeroelastic instability onset by means of run-away analyses, followed by the conclusions.

2. Modeling

The reference for the tool comparison in this work is a HAWC2 model of the IWT-7.5-164 wind turbine. Its current revision 4.0 together with a specification of the turbine characteristics is publicly available [20]. The model in this study differs from this version in certain aspects: the airfoil polars are interpolated to a specific Reynolds number distribution along the blades, aerodynamic drag on the nacelle is not considered and the drive train is assumed to be rigid.

For the objectives of this study the HAWC2 reference model is translated for the simulation tools alaska/Wind, Bladed, OpenFAST and Simpack. On one hand differences between the simulation models are caused by different modeling capabilities of the tools. As a consequence, not always a one-to-one relation could be realized. On the other hand one goal is to investigate the impact on the aeroelastic properties, that arises from different modeling techniques. Thus, for each of the tools a typical configuration is chosen, even though the tool might offer additional modeling features. Table 1 summarizes the variety of modeling techniques in the comparison.

The main differences appear in the structural models. These are in a range from linear single body modal models to geometrically exact finite beam element formulations (GEBT, [22]). The blade models in alaska/Wind, Ansys®[23], HAWC2 and OpenFAST use 6x6 mass and stiffness matrices as inputs. Alaska/Wind and OpenFAST solve the nonlinear FE-beams for the blades in time domain, while HAWC2 uses a multi-part modal reduction approach. Bladed takes into

Table 1. Overview of the modeling techniques used in the comparison

Model	alaska/Wind	Bladed	HAWC2	OpenFAST	Simpack
Version	9.6	4.9	12.8	2.2.0	2019x.2
Tower structure	Modal[1], MD	Modal[1], MD	Modal[1], RD	Modal[1], MD	Modal[2], MD
Blade structure	FE[3], RD	Modal[1], MD	Modal[4], RD	FE[1,3], RD	Modal[2], MD
Rotor aerodynamics	BEM, BL, DF	BEM, BL, ODW	BEM, BL, DI	BEM, BL	BEM, BL

FE: *Finite Elements* MD: *Modal Damping* RD: *Rayleigh Damping*
[1] *single body, internal Finite Element Analysis (FEA)*
[2] *single body, external FEA*
[3] *internal model based on* 6×6 *mass and stiffness matrices*
[4] *multi-body, internal FEA*
BEM: *Blade Element Momentum theory* BL: *Beddoes-Leishman dynamic stall model*
DF: *Dynamic Flex wake model* ODW: *Øye Dynamic Wake model* DI: *Dynamic Inflow model*

account only specific cross section data out of the full matrices and within this study only the single part modal reduction is used. Simpack uses the condensed modal model out of Ansys® to define the elastic blade body. Furthermore, the tools apply different models for the structural damping. The reference HAWC2 model provides a logarithmic decrement for each of the tower and blade modes. These are used to compute damping coefficients for the other models. For tools that rely on a Rayleigh damping model there is no direct match and the (stiffness-proportional) coefficients are chosen in a way that the eigenfrequencies of the first two bending modes agree to the reference.

All aerodynamic models are based on the (quasi-steady) blade element momentum theory (BEM), accompanied by separate models for dynamic stall and wake effects. Each of the tools has a specific BEM implementation, while OpenFAST and Simpack both include the AeroDyn library in version 15 [24] and 13 [25], respectively. In the dynamic test cases shown in this article OpenFAST and Simpack are used without the dynamic wake models of their AeroDyn versions, since they do not produce reliable results or destabilize the numerical simulation for the models in this comparison.

3. Model verification

The model verification is made through a sequence of test cases with increasing complexity, ranging from the structural properties of the tower and the blades to the dynamic response of the wind turbine. A selection of the corresponding results is shown here. Ansys® is used as benchmark reference for the structural tests as it is a validated and recognized reference for structural modeling just as HAWC2 for the aeroelastic tests as it also served as reference for the modeling in the other simulation tools.

The blade mass, center of gravity position and modal parameters are compared to verify a correct implementation of the blade structure. The blade mass and c.o.g. are in good agreement with deviations well below 1 %. The first 12 eigenfrequencies of the isolated blade are listed in Table 2. The overall agreement is satisfying. The most noticeable differences are the first and second torsion modes in Bladed, with a deviation up to 10% with respect to the Ansys® model. Furthermore, the eigenfrequencies in alaska/Wind are consistently slightly lower than the other tools, but stay in acceptable bounds.

3.1. Static blade deformations

The static structural behavior of the blade is verified by static deformation tests. Therein, the blade is fixed at the root and the length axis points parallel to the ground. Quintuple gravitation

Table 2. Comparison of blade eigenfrequencies, reference = Ansys®

Mode	Ansys®(f/Hz)	Bladed	HAWC2	HAWCStab2	Simpack	alaska/Wind
1st flap	0.66	-0.7%	-0.7%	-0.3%	0.0%	-1.4%
1st edge	0.99	-0.1%	-0.7%	-0.2%	0.0%	-3.6%
2nd flap	1.76	-0.3%	-0.7%	-0.2%	0.0%	-2.5%
2nd edge	2.98	-0.0%	-0.9%	-0.4%	0.0%	-4.2%
3rd flap (+edge)	3.57	-0.4%	-0.7%	-0.2%	0.0%	-3.3%
4th flap (+edge)	5.93	-0.4%	-0.9%	-0.5%	0.0%	-3.3%
3rd edge	6.27	-0.3%	-0.8%	-0.3%	0.0%	-4.0%
1st torsion	8.77	-11.3%	-0.4%	-0.1%	0.0%	-0.2%
5th flap	9.04	-0.6%	-1.2%	-0.7%	0.0%	-3.2%
4th edge	10.77	-0.4%	-0.8%	-0.3%	0.0%	-3.5%
6th flap	12.52	-0.7%	-0.8%	-0.4%	0.0%	-3.1%
2nd torsion	14.22	-9.9%	-0.1%	0.2%	0.0%	-0.3%

is applied in two different orientations rotated around the length axis: a) The suction side facing downwards, i. e. the main load direction is flapwise. b) The leading edge facing downwards, i. e. the main load direction is edgewise.

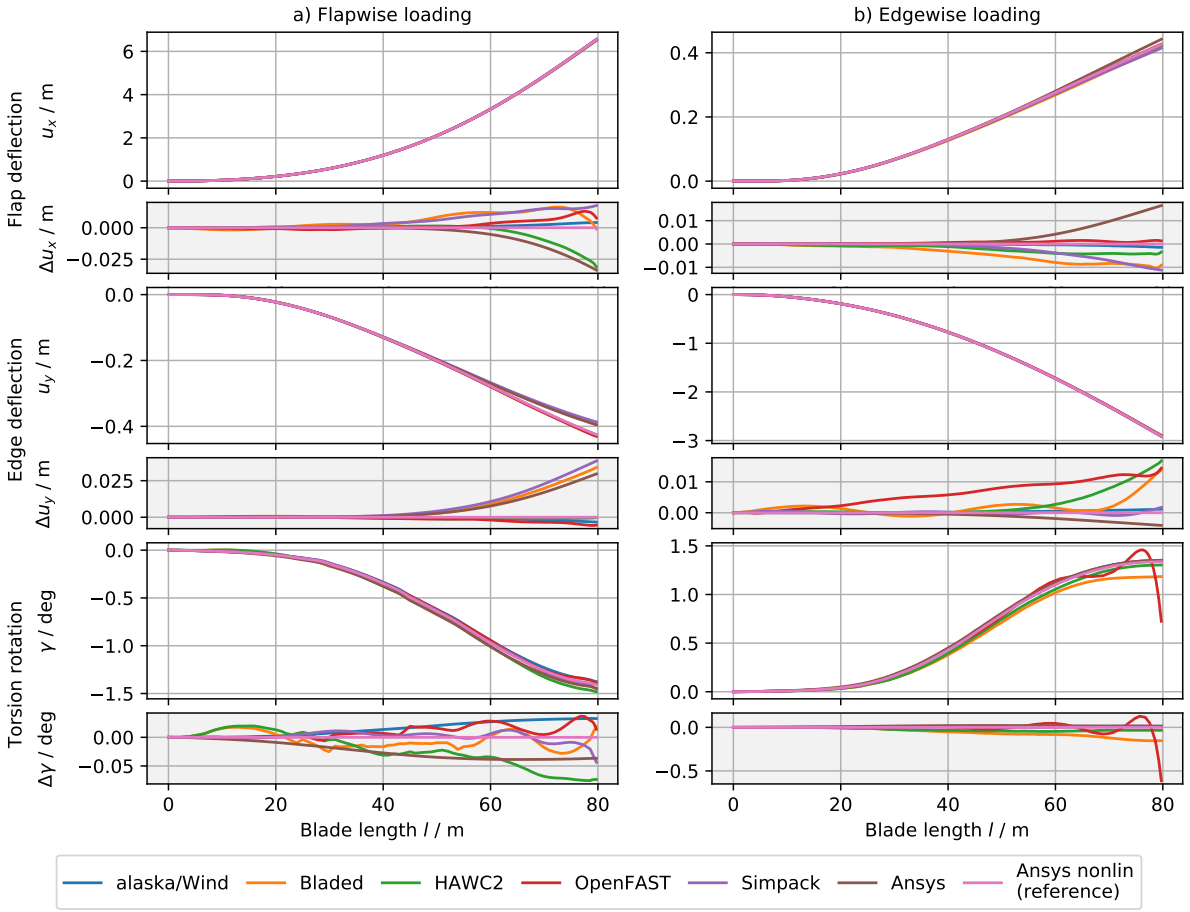

Figure 1. Deformations under static quintuple gravitation acting in flapwise (left column) and edgewise (right column) direction

The flapwise, edgewise and torsional deflections are shown in Fig. 1. Each deflection is visualized both in magnitude and as an absolute difference with respect to the non-linear Ansys®model. The deflections in the main load direction are in excellent agreement. Noticeable disagreements appear in the coupled deflection directions. Two clusters in the models can be distinguished in the coupled edgewise deflection under the flapwise loading. The tools based on a linear elastic model (Bladed, Simpack and linear Ansys®) deflect significantly less than the other models which include non-linear effects. The clusters are not so clear in the coupled flapwise deflection under the edgewise loading, but the linear models show again the largest disagreement with respect to the non-linear Ansys®reference result. The largest relative deviation between the tools is found in the torsional deformation. There is no unambiguous dependency on the (non-)linearity of the models. The Bladed results show the largest discrepancy, which correlates to the deviations of the torsional modes in the eigenvalue analysis. For OpenFAST the reason for the oscillation in torsion near the tip is likely an internal cubic spline fit of BeamDyn that leads to an incorrect calculation of the blade curvature and incorrect capture of the twist at the tip of the blade [26].

Overall, the agreement for the static blade deformation test is satisfactory. The differences between the linear and non-linear approaches are explainable. The largest disagreements occur in the torsional deformation, which has been expected.

3.2. Steady state aeroelasticity

The steady state aeroelastic test combines flexible blades with steady state aerodynamic loading at rated wind speed conditions. Apart from the blades, the turbine is modeled with rigid components and does not include any asymmetries. The rotor speed is set to 10 rpm. Gravitation is not included. The wind field is uniform and stationary. The wind velocity is $10\,\mathrm{m\,s^{-1}}$. A steady state and purely aerodynamic test with a fully rigid turbine, which has been conducted earlier, has shown no discrepancies in the aerodynamic models. The steady state aeroelastic forces, moments and deformations are shown in Fig. 2. The absolute differences are given with respect to HAWC2. The aerodynamic forces, both in in-plane and out-of-plane direction, are in excellent agreement, as well as the torsional moment. Corresponding to the findings of the purely structural deformation test, the non-linear structural models are in close proximity in the in-plane and out-of-plane deflection, while the linear models (Simpack and Bladed) show a noticeable deviation. Again, the torsional deformation shows the largest variation between the tools with absolute differences exceeding 0.5°. The excellent agreement in aerodynamic loads, but relatively larger deviations in the deflections shows the dominating uncertainty in structural modeling, especially introduced by the structural coupling, for static aeroelastic cases.

3.3. Periodic dynamic aeroelasticity

The dynamic structural and aeroelastic behavior of the wind turbine models is verified by a test case with a periodic unsteadiness. The blades are the only flexible component, the rotor speed is constant at 10 rpm and the gravitational loading is the only model asymmetry. The dynamic structural test does not include the aerodynamic forces, while the dynamic aeroelastic test incorporates a constant $10\,\mathrm{m\,s^{-1}}$ wind speed.

Fig. 3 shows out-of-plane and in-plane deflections and the angle of attack (AOA) of a blade section at 57 m radius as a function of the rotor azimuth, with 0° azimuth defined as the position where the blade points upwards. The top row is the answer of the purely structural model, the bottom row shows the results of the aeroelastic model. The emphasis in this test case lies on the amplitude and phase of the oscillations, rather than the mean value. Note that the mean values of the dynamic aeroelastic test correspond well to the steady state results in Fig. 2. The in-plane deflection, as main direction of the unsteady gravitational load, shows no notable amplitude or phase differences both in the structural and aeroelastic test. However, discrepancies arise in

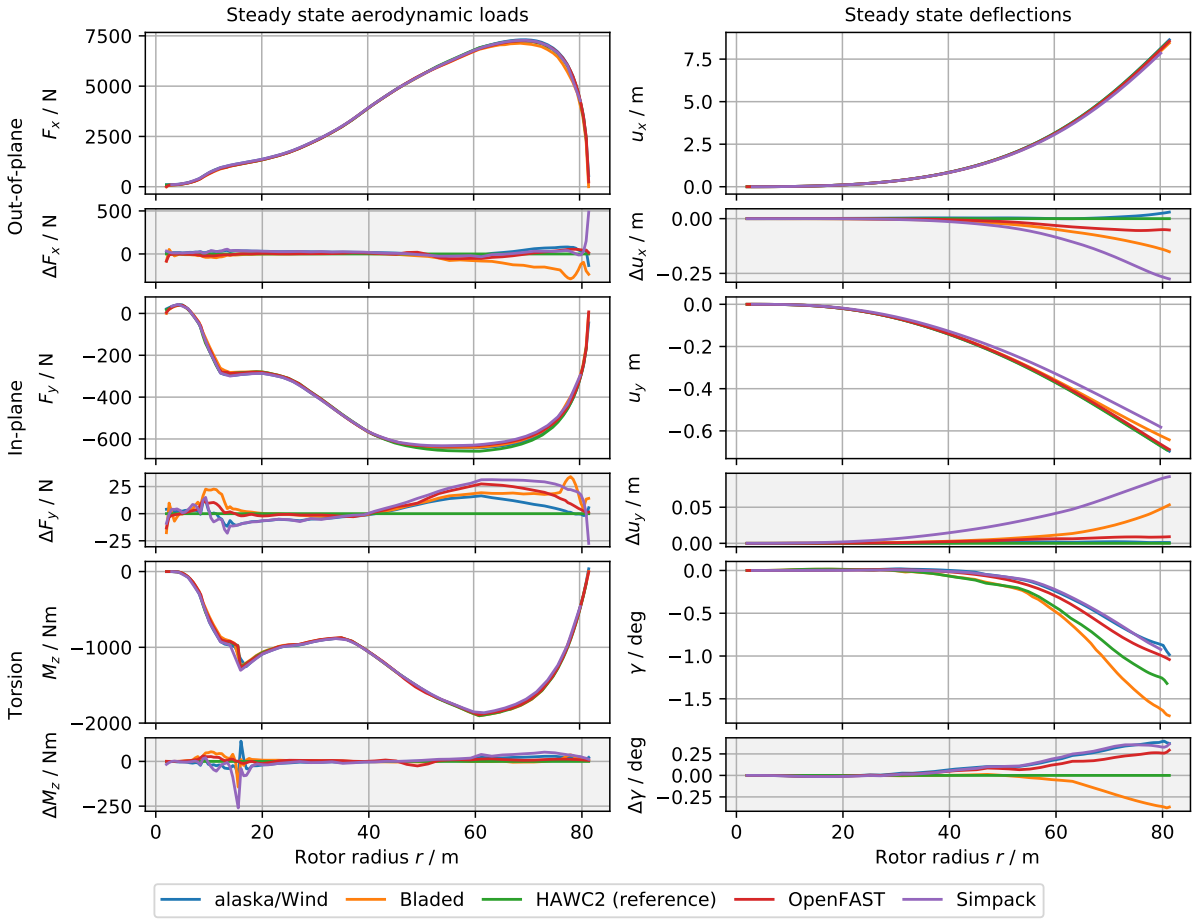

Figure 2. Steady state aeroelastic loads and deformations ($10\,\mathrm{m\,s^{-1}}$ wind velocity)

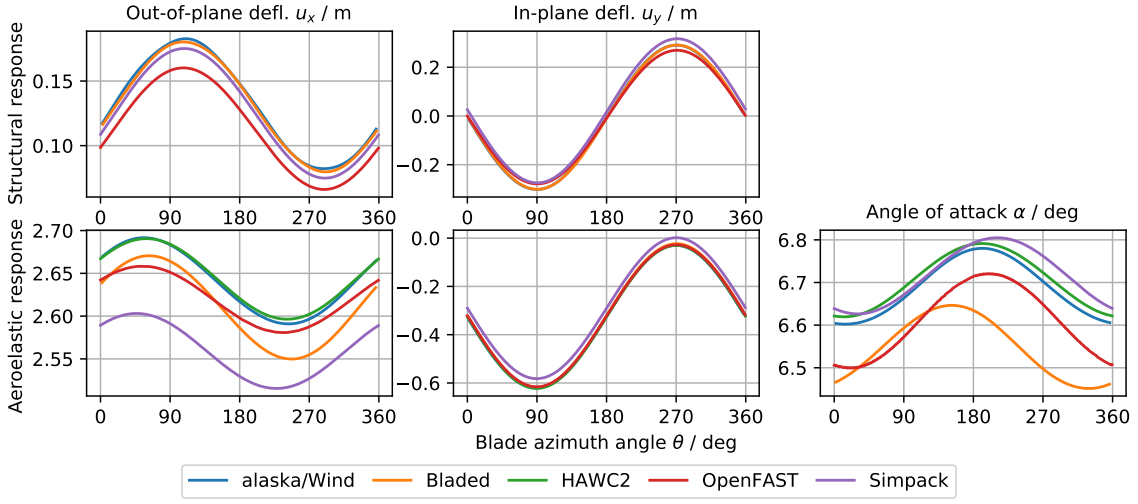

Figure 3. Periodic dynamic structural (top) and aeroelastic (bottom) response ($r = 57\,\mathrm{m}$)

the out-of-plane deflection for the aeroelastic test case. The out-of-plane amplitudes vary from 3.9 cm to 6.0 cm and there is a phase difference of about 20° between Bladed and Simpack for the aeroelastic test. The discrepancies are related to differences in the aerodynamic loads that are again impacted by the AOA, where Bladed and Simpack are separated by a phase shift of approximately 60°.

The comparison of the dynamic structural and dynamic aeroelastic verification tests shows that the main discrepancy factor are the aerodynamics. This is in contrast with the static aeroelastic tests, where the structural modeling was the main cause of differences. It is evident that the discrepancies in this periodic test case are significant. The root causes are not yet identified and need to be further investigated. The presence or absence of a dynamic wake model (OpenFAST and Simpack are executed without such a model) is not decisive though.

4. Run-away simulations

This section discusses the code-to-code comparison of the run-away analysis. The aim is to investigate the onset of aeroelastic instability with the different simulation tools.

The blades and the tower are flexible in this case, but the drive train is still rigid. The conditions are forced to be as symmetrical as possible, i.e. gravity, tilt angle, wind shear and tower shadow are disabled. However, the deformation of the tower yields an inclination of the rotor, resulting in a harmonic excitation of the blades similar to a tilt angle. The wind speed is ramped up at a constant rate of $0.0115\,\mathrm{m\,s^{-2}}$ until the turbine becomes unstable or the numerics do not converge anymore. Fig. 4 shows the resulting rotor speed and out-of-plane deflection at 57 m blade radius versus the wind velocity. The time series of only two representative turbine parameters are shown because the important and observable characteristics are similar for all available sensors.

The point of instability onset is defined here as the wind speed at which the rotor speed stops increasing or suddenly drops [14]. The instability onset usually takes place in parallel with excessive oscillations of the blades and tower, since part of the rotational energy is transferred into the instability. The onset points are indicated in Fig. 4 by the dashed lines. It is obvious that

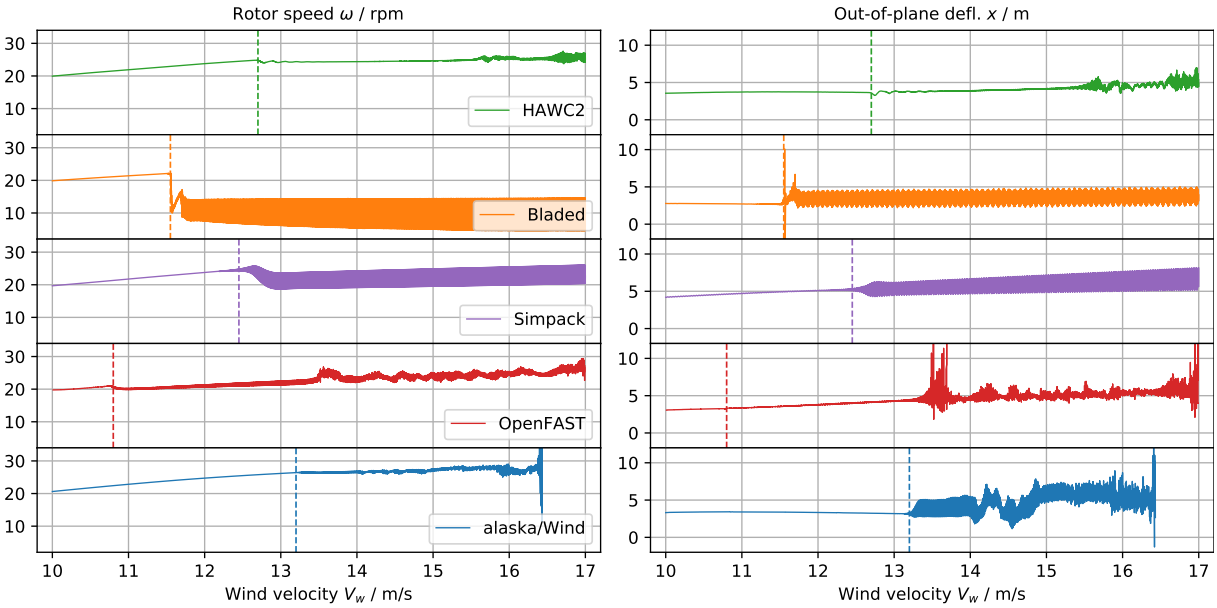

Figure 4. Run-away analysis: Rotor speed and out-of-plane deflection at 57 m blade radius as a function of the linearly increasing wind velocity

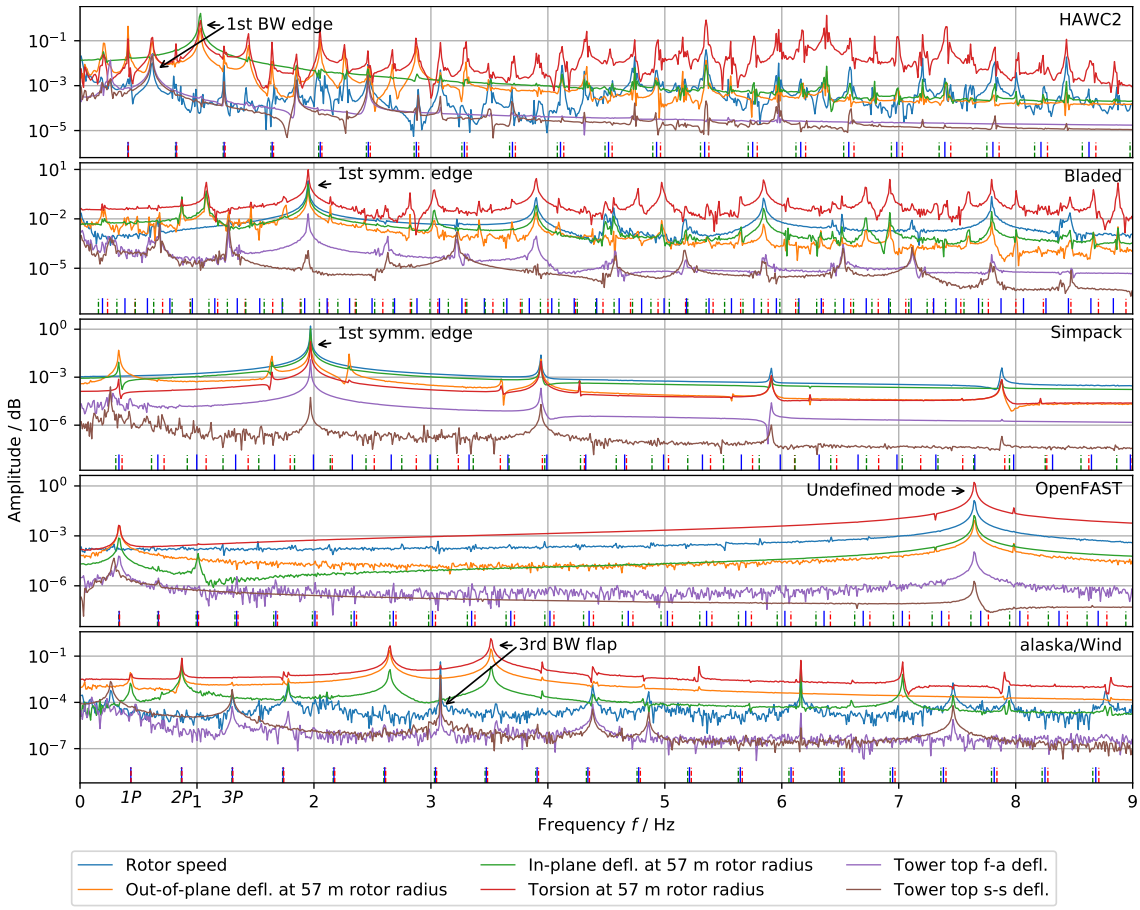

Figure 5. Amplitude Fourier spectrum at constant wind speed

there is a significant variance on the instability onset between the tools. The first instability occurs in OpenFAST at a wind speed of approx. $10.8\,\mathrm{m\,s^{-1}}$ and the last in alaska/Wind at $13.2\,\mathrm{m\,s^{-1}}$. The graphs also show a large variation in the qualitative vibration behavior in the unstable regime, ranging from well organized and rather harmonic vibrations (Bladed and Simpack) to more stochastic and chaotic vibrations (OpenFAST, HAWC2 and alaska/Wind).

Two methods were pursued to give insight in the instability mechanism. First, the time domain data are mapped to the frequency domain by means of a Fast Fourier Transformation (FFT). Therefore the analysis was repeated with a step-wise increase of the wind velocity (steps of $0.1\,\mathrm{m\,s^{-1}}$, duration of 200 s). The amplitude spectra of the rotor speed, tower top fore-aft and side-to-side motion in the non-rotating frame as well as the spectra of the out-of-plane deflection, the in-plane deflection and torsion at 57 m blade radius in the rotating blade reference frame are shown in Fig. 5. Besides the spectra, rotor harmonics are indicated at the bottom of each plot. Because the rotor speed is not constant along the full time window used for the FFT, the excitation harmonics might have a spread, which depends on the instability behavior as predicted by the respective tool. This is indicated by the dashed, green and red lines. They represent the minimum and maximum frequency of each rotor harmonic. Secondly, the results of the run-away simulations are compared with a linear frequency domain analysis in HAWCStab2, see Campbell diagram in Fig. 6, and with the eigenvalue analysis presented in section 3.

Based on the information of a visualization (that was preliminarily investigated), FFT and HAWCStab2 linearization, four main instability mechanisms are observed.

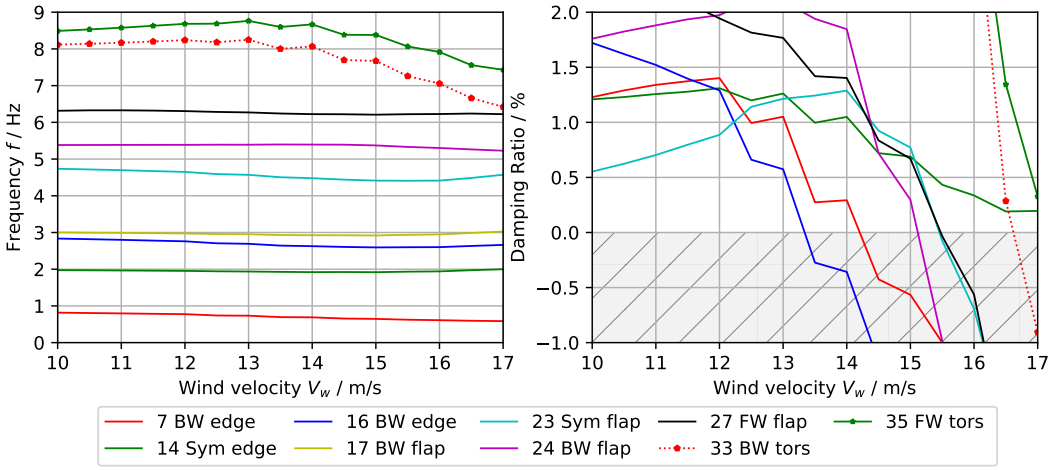

Figure 6. HAWCStab2 linearization result: selected negative and relevant low damped modes

The instability mechanism in HAWC2 corresponds to the *first edgewise backwards whirling* mode with a strong participation of the first torsion mode. This instability was clearly identified in an animation of the HAWC2 time series data. The peak in the frequency spectrum of the blade deformations at approximately 1 Hz corresponds to the eigenfrequency of the first edgewise mode of the isolated blade, as listed in Table 2. The corresponding peaks in the rotor speed and tower deformations (inertial frame) can be identified at approximately 0.6 Hz, exactly one rotor harmonic less ($\pm\Omega$). This confirms that this instability can be denominated as the first edgewise backward whirling mode. The HAWCStab2 linearization is in excellent agreement with this finding. The first edgewise backwards whirling mode is situated in the same frequency range for the considered wind speeds and the damping of this mode becomes negative.

The second instability phenomenon is observed both in Simpack and Bladed and is related to the *first symmetric edgewise* rotor mode. An animation of the simulation results shows an in-phase blade deformation of the three blades dominated by the first edgewise bending mode. Furthermore, the dominating frequency in the Fourier spectrum is located at approximately 2 Hz, which agrees with the HAWCStab2 linearization result for the symmetric edge mode. This same mode has a low, but non-negative damping in the linearization. The peak in the frequency spectrum is located at the same point for both the signals in the rotating reference frame and those in the inertial reference frame. This supports the indication of a symmetrical rotor mode.

The Fourier spectrum of OpenFAST shows the strongest peak at approx. 7.7 Hz. This mode has a large torsional participation, but a corresponding mode could not be found in the linearization or in the eigenanalysis. The identification of this instability mechanism will be a subject of future investigations.

The final instability phenomenon is only observed in the alaska/Wind results. The *third flapwise backward whirling* mode, with a large participation of the second edgewise bending and the first torsional mode, has a dominating participation in the instability. The corresponding peaks in the rotating frame at 3.5 Hz and in the standstill frame at 3.1 Hz are in good agreement with the 3rd flapwise mode of the isolated blade.

Altogether the results differ significantly. The predicted instabilities occur at different wind speeds (thus operating points) and different mechanisms are observed. Discrepancies in verification test cases indicate that the dynamics of the aeroelastic systems are not captured in the same way. The test cases do not cover the full complexity of the problem though, so that

they are not sufficient to explain the observed differences in detail. It is worth to mention, that time series data could be matched successfully with linearization results across the tools in many simulations.

5. Conclusions and Outlook

The code-to-code comparison showed that the agreement between the state-of-the-art tools varies with the complexity of the aeroelastic test cases. Only minor deviations are found in the static deformation tests and in the steady state aeroelastic simulation. These discrepancies are caused by the differences in the modeling of the structural coupling. There is a clear difference between the linear and non-linear structural models and the largest differences appear in the torsional deformation. Major discrepancies appear when dynamic effects are taken into consideration. The unsteady aerodynamic modeling is identified as the main cause for discrepancies. The analysis of the run-away simulation shows the further complexity involved in stability prediction. The investigated tools differ significantly both in the estimation of the instability point as in their prediction of the manifesting instability mechanism. The underlying reasons for the differences are not fully understood and will be a subject of further research. Therein, the authors will investigate the influence of modeling uncertainties on stability predictions of the aeroelastic simulation tools in order to identify the most influential parameters and to define more relevant test cases accordingly. Further research is also required to understand the impact of the unsteady aerodynamic modeling on the stability prediction. Special attention should be paid on the dynamic wake modeling, turbulent wake state correction and dynamic stall models.

Acknowledgments

This work is a collaboration of four partners from research and industry in the frame of work package 4.2 of the German national research project *SmartBlades2*. This project is funded by the German Federal Ministry for Economic Affairs and Energy, grant no. 0324032 A/C.

References

[1] Veers P *et al.* 2019 *Science* **366**
[2] Jonkman J and Musial W 2010 Offshore Code Comparison Collaboration (OC3) for IEA Wind Task 23 Offshore Wind Technology and Deployment Tech. rep. NREL, Golden
[3] Jonkman J, Butterfield S, Musial W and Scott G 2009 Definition of a 5-MW Reference Wind Turbine for Offshore System Development Tech. rep. NREL, Golden
[4] Simms D, Schreck S, Hand M and Fingersh L J 2001 NREL Unsteady Aerodynamics Experiment in the NASA-Ames Wind Tunnel: a Comparison of Predictions to Measurements Tech. rep. NREL, Golden
[5] Hodges D H and Pierce G A 2011 *Introduction to Structural Dynamics and Aeroelasticity* (Cambridge University Press)
[6] Hansen M H 2007 *Wind Energy* **10** 551–577
[7] Lobitz D W 2004 *Wind Energy* **7** 211–224
[8] Hansen M O L *et al.* 2006 *Progress in Aerospace Sciences* **42** 285–330
[9] Bir G and Jonkman J 2007 *J. Phys.: Conf. Series* vol 75
[10] Hansen M 2003 *Wind Energy* **6** 179–195
[11] Hansen M 2004 *42nd AIAA Aerospace Sciences Meeting and Exhibit* p 505
[12] Skjoldan P F and Hansen M H 2012 *Wind Energy* **15** 275–287
[13] Bottasso C L and Cacciola S 2015 *Wind Energy* **18** 865–887
[14] Pirrung G R, Madsen H A and Kim T 2014 *J. Phys.: Conf. Series* vol 524
[15] alaska/Wind by IfM Chemnitz, Version 9.6
[16] Dassault Systèmes Simpack, Version 2019x.2
[17] DNV-GL®Bladed, Version 4.9
[18] Larsen T J and Hansen A M 2007 How 2 HAWC2, the User's Manual Tech. rep. Risø National Laboratory
[19] OpenFAST v2.2.0 web page `https://github.com/OpenFAST/openfast` accessed: 2019-11-13
[20] Popko W *et al.* 2018 IWES Wind Turbine IWT-7.5-164. Rev 4 Tech. rep. Fraunhofer IWES
[21] Teßmer J *et al.* 2016 Final Report: Smart Blades Tech. rep. German Aerospace Center (DLR)
[22] Hodges D H 2006 *Nonlinear composite beam theory* (AIAA, New York)

[23] Ansys® Academic Research Mechanical, Release 19.1
[24] NWTC Information Portal (AeroDyn). https://nwtc.nrel.gov/aerodyn. Last modified May 25 2017, accessed Feb. 29 2020
[25] NWTC Information Portal (AeroDyn v13). https://nwtc.nrel.gov/aerodyn13. Last modified Sept. 23 2015, accessed Feb. 29 2020
[26] Reference to known issues in BeamDyn `https://github.com/OpenFAST/openfast/issues/366` accessed: 2020-02-28